Available online at www.sciencedirect.com
ScienceDirect
Chemical Engineering and Processing 47 (2008) 1150–1158
Chemical Engineering and Processing Process Intensification
www.elsevier.com/locate/cep

Droplet detachment in cross-flow membrane emulsification: Comparison among torque- and force-based models

Giorgio De Luca [a,*], Francesco P. Di Maio [b], Alberto Di Renzo [b], Enrico Drioli [a]

[a] *Research Institute on Membrane Technology (ITM-CNR), via P. Bucci, Cubo 17C, 87036 Rende (CS), Italy*
[b] *Dipartimento di Ingegneria Chimica e dei Materiali, Università della Calabria, via P. Bucci, Cubo 44A, 87036 Rende (CS), Italy*

Received 10 December 2006; received in revised form 7 February 2007; accepted 23 March 2007
Available online 4 April 2007

Abstract

Due to the high product quality achievable, considerable attention of the researchers is being addressed to the cross-flow direct membrane emulsification (CDME). The key advantages of this process over traditional technologies are a better control of the droplet sizes of the emulsion and its efficiency in terms of energy density requirement. In the literature, macroscopic models have been employed to describe the influence of process parameters and membrane properties on droplet formation. These models have been based either on an algebraic torque balance equation (TBE) or on a force balance (FBE) along a contact line, defined on the droplet pore border. The aim of this work is to compare the results obtained using these two approaches against experimental data available in literature in order to assess the reliability in predicting the correct trends with good quantitative agreement. The analysis shows that FBE yields better results than TBE under conditions of wall shear stress equal or larger than 7 Pa and membrane pore diameters below 1.5 μm. In the mentioned conditions, using the FBE model, the maximum error in predictions is around 10%. Both methods reproduce the empirical relationship between droplet sizes and cross-flow velocities, although the force balance yields a better behaviour (plateau) for high wall shear stresses. However, the analysed models are unable to reproduce the linear relation between the droplet and pore size observed in the experiments.

Keywords: Membrane emulsification; Droplet detachment; Torque balance modelling; Force balance modelling

1. Introduction

Emulsions are generally disperse systems of two (or more) immiscible liquids in which one phase (disperse phase) is distributed in form of droplets in the other phase (continuous phase). These systems are commonly encountered in key processes, e.g. in the pharmaceutical and food industry as well as in cosmetic products. Both the average droplet size and size distribution are very important properties, since they determine the emulsion stability and its properties for the intended uses. For large-scale emulsion production the most commonly employed methods are based on techniques aiming at establishing a turbulent regime (turbulent eddies) in fluid mixtures. According to the known techniques, the size of droplets, for a given pair of processed phases, is mainly determined by the size of the turbulent eddies and the times of exposure [1]. However, these turbulent flows cannot be controlled or generated uniformly in the mixture. The consequences are that wide size distributions are commonly obtained and energy is used inefficiently. In addition, the behaviour of any pair of immiscible phases cannot be predicted on a large-scale, based on the tests performed in the laboratory; therefore, process scale-up is extremely difficult. Recently, more attention has been addressed to an alternative emulsification process, i.e. the membrane emulsification (ME). A valuable advantage in membrane emulsifications is that droplet size distributions can be carefully and easily controlled, since the size of the droplets is directly related to the size distribution of the membrane pores. Therefore, product properties can be tuned by simply choosing suitable membranes and adapting the key process parameters. Membrane emulsification is also an efficient process, since the energy density requirement (energy input per cubic meter of emulsion produced) is low with respect to other techniques, especially for emulsions with droplet diameter smaller than 1 μm [1]. Moreover, in conventional emulsification methods, the high shear rates and the resulting increase of the process temperature have negative effects on shear- or

* Corresponding author. Tel.: +39 0984 49 2027; fax: +39 0984 40 2103.
E-mail address: g.deluca@itm.cnr.it (G. De Luca).

0255-2701/$ – see front matter © 2007 Elsevier B.V. All rights reserved.
doi:10.1016/j.cep.2007.03.010

temperature-sensitive components; as a result, the lower energy density requirement also improves the quality and functionality of delicate emulsion ingredients.

Membrane emulsifications can be generally distinguished in: (i) pre-mix membrane emulsification, in which a coarse pre-mixed emulsion is compressed through the membrane pores to reduce the droplet sizes, and (ii) direct membrane emulsification (DME), in which the disperse phase is directly fed through the membrane pores to obtain droplets. The cross-flow membrane emulsification (CDME) represents a direct membrane emulsification, in which the droplets, formed at the pore mouth (on the membrane surface), grow until a critical dimension and then are carried away with the continuous phase, flowing parallel to the membrane surface. Very regular mono-disperse droplets can be obtained, though the emulsions with droplet diameters above 0.1 μm generally require additional substances acting as emulsifiers. The droplet size in CDME depends on several parameters, the most important are: (i) trans-membrane pressure, which affects the flux of disperse phase through the membrane pores, (ii) continuous phase cross-flow velocity, (iii) membrane pore size and morphology, (iv) wetting property of the membrane surface and (v) dynamic interfacial tension. On the experimental side, the influence of the parameters on the emulsion properties have been investigated [2–5] and two important relationships have been well established. A linear scaling law has been generally observed between the droplet size and the membrane pore size with a slope ranging typically from 2 to 10, although values up to 50 have also been found [6]. Secondly, a hyperbolic-like correlation between the emulsion droplet diameter and the cross-flow continuous velocity has also been established [2,3,5].

From a theoretical point of view, droplet formation during CDME has been described using models different in the scale or in the considered mathematical and physical phenomena: microscopic modelling has been performed using (i) computational fluid dynamics (CFD) [1,7], (ii) surface free-energy minimization [8,9] and recently (iii) lattice Boltzmann [10]. Overall force and torque balances on the droplet also provided interesting results in terms of reproducing the actual properties of the emulsified phase [3,11,12]. These global balance models are less accurate than the methods at smaller scales; on the other hand, they are useful in optimization studies as well as easier to handle and more instructive. The latter feature is crucial to acquire the necessary understanding of the physical causes at the basis of the droplet formation and detachment. In addition, these methods are easily versatile, allowing to analyse the influence of many processes and membrane parameters with limited computational efforts. Until now, the proposed approaches to describe the droplet formation during CDME make use of either an algebraic torque balance equation (TBE) [3] or a force balance (FBE) along the droplet contact line located around the membrane pore border [12]. However, a reliable theoretical model capable of describing and predicting the empirically observed trends has not been formulated yet.

In the current work, we briefly illustrate the properties and main assumptions of the TBE and FBE models (Section 2). We compare the results obtained from the balance approaches with particular focus on the prediction capabilities in terms of both the aforementioned empirical relationships and the order of magnitude of the droplet diameters. The results are compared with some experimental data available in the literature with the aim to show in which conditions the balance-based models can be considered reliable (Section 3). We close in Section 4 with some conclusions.

2. Droplet detachment models

Prior to describing the details of each set of balance equation, let us discuss the macroscopic forces acting on the droplet considered in a similar way in both models. In the following subsections, we examine the force considered differently in the two models, i.e. the surface tension force.

Let us consider a droplet during its growth on the pore outlet (Fig. 1). The forces acting on the droplet can be conveniently subdivided into perpendicular and parallel direction with respect to the membrane surface. Considering the former case, the Young–Laplace force F_{YL} [6,11], dynamic lift F_{DL} and buoyancy force F_{BG} [6,11] are taken into account. They are defined as:

$$F_{YL} = \frac{\gamma}{D_d}\pi D_p^2 \tag{1}$$

$$F_{DL} = 0.761\frac{\tau_{c,s}^{1.5}\rho_c^{0.5}}{\mu_c}D_d^3 \tag{2}$$

$$F_{BG} = \frac{1}{6}\pi g\,\Delta\rho D_d^3 \tag{3}$$

where D_p and D_d correspond to the average membrane pore and droplet diameter, respectively, γ the liquid–liquid interfacial tension, while $\tau_{c,s}$, ρ_c and μ_c represent the wall shear stress, density and viscosity of the continuous phase, respectively. The quantity $\Delta\rho$ in Eq. (3) represents the difference between the

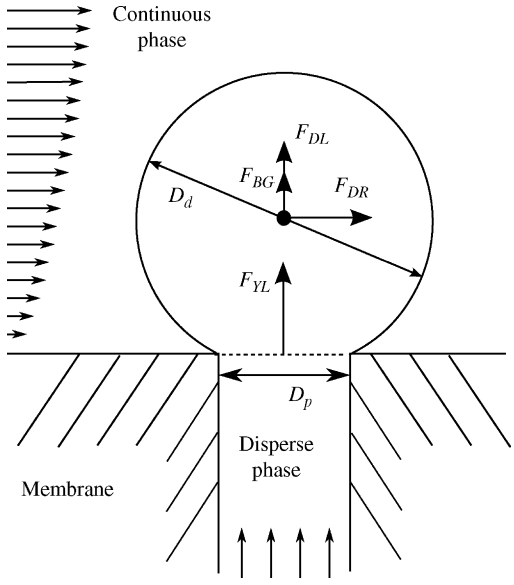

Fig. 1. Main macroscopic forces acting on the droplet stuck on the membrane pore border. The direction of buoyancy is illustrative, the real one depends upon the geometry and orientation of the membrane module.

continuous and disperse phase densities. In Fig. 1, only one possible direction of the buoyancy force (F_{BG}) is sketched, while in general the direction of F_{BG} depends on the geometry and orientation of the membrane module. However, various authors (e.g. [6,12]) showed that, in the conditions considered in the present work, F_{BG} is negligible. The drag force F_{DR} [3,6,11] due to continuous phase cross-flow and parallel to membrane surface is defined as:

$$F_{DR} = \frac{3}{2} k_x \pi \tau_{c,s} D_d^2 \tag{4}$$

where the parameter k_x is equal to 1.7 and takes into account the wall correction factor for a single sphere touching an impermeable wall [13]. In Eq. (4), the approximation $v\mu_c \approx (1/2)\tau_{c,s} D_d$ is adopted, where v is the undisturbed cross-flow velocity, and the shear stress, evaluated at the droplet centre, is assumed equal to the one at the membrane surface, i.e. $\tau_{c,s}$.

The inertial force due to the flow of the disperse phase would be another force contribution to consider. However, it is important to remark that in process conditions ensuring mono-disperse droplets and without jets of the disperse phase the trans-membrane pressure is never markedly higher than the Young–Laplace critical pressure of the system. In these conditions, the corresponding disperse phase flux through the membrane pores produces a negligible inertial force.

The forces considered above have to be counterbalanced by the action of the interfacial tension along the droplet–pore contact line. A different approach to account for this force is used in the TBE and FBE models and these will be discussed separately in the following subsections.

2.1. Torque balance equation

In the commonly used torque balance model, as proposed by Peng and Williams [3], the droplet is considered as a rigid spherical cap subjected to the forces discussed above (Fig. 2a). To be able to calculate the instant when the droplet has sufficiently grown to detach from the pore, Peng and Williams [3] suggested a torque balance around the foremost point on the pore circumference (point A in Fig. 2a). This allows to calculate at what diameter of the growing droplet torques in clockwise and anticlockwise directions are balanced, implying that past this value the drop would roll, i.e. detach from the membrane.

If we consider a uniform interfacial tension along the droplet contact line, causing a force [6] defined as:

$$F_\gamma = \pi D_p \gamma \tag{5}$$

and cast the torque balance around the pole, we end up with the following equation:

$$F_{DR}\left[h - \frac{D_d}{2}\right] = (F_\gamma - F_{YL} - F_{DL} - F_{BG})\frac{D_p}{2} \tag{6}$$

Once the system geometry, continuous and disperse phase properties and membrane characteristics (average pore size, wetting) are known, Eq. (6) results in an algebraic equation in D_d that can be easily solved to find the desired drop diameter. For a given pore diameter D_p, Eq. (6) has two real solutions. The smallest one is always similar to D_p whatever the interfacial tensions and shear stresses values are used. This fact is not physically consistent, thus such solution will not be considered in the results presented below.

2.2. Force balance equations

Let us consider a *deformable* droplet during its growth on the pore outlet (Fig. 2b). The starting point of the FBE model is that this droplet grows leaning on the pore border as long as a force equilibrium exists along its contact line [12]. The drop deformability is taken into account through the evaluation of the advancing and receding contact angles along the droplet–pore contact line. In these conditions, the detachment is supposed to occur when the interfacial force at the droplet base is unable to counterbalance, through the droplet inclination, the actions mainly due to the continuous fluid cross-flow and Young–Laplace force. As a consequence, the droplet connection to the liquid in the pore fails. From another point of

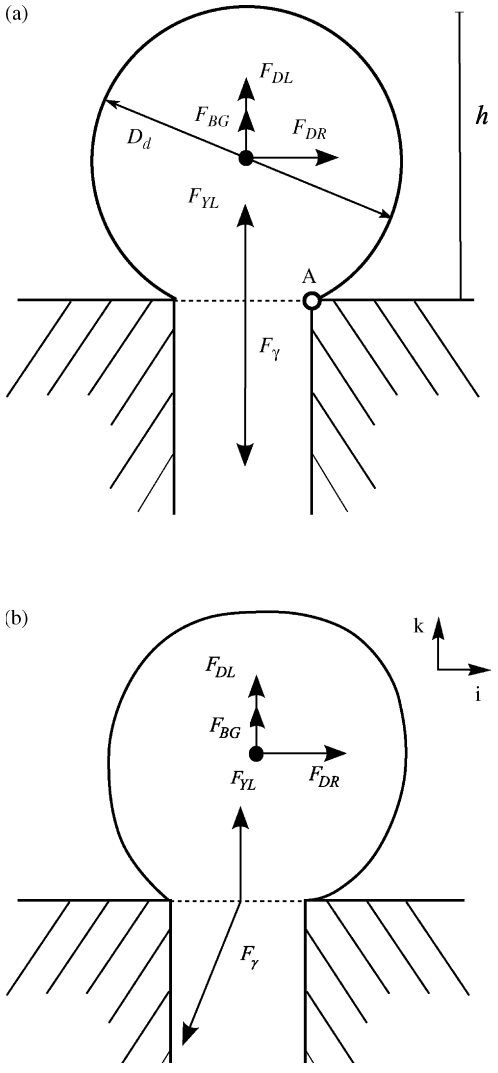

Fig. 2. Macroscopic surface tension force, F_γ, as considered in the TBE (a) and FBE (b) models. The direction of buoyancy is illustrative, the real one depends upon the geometry and orientation of the membrane module.

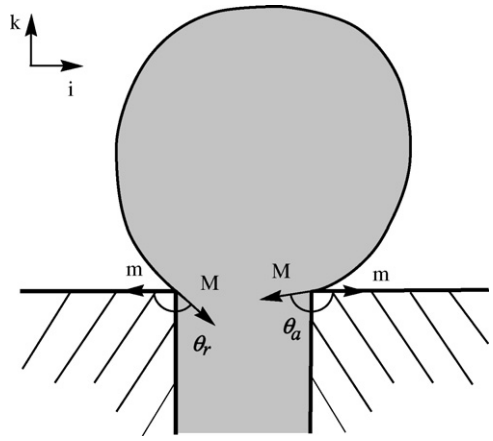

Fig. 3. Droplet formation at the pore outlet. Side view indicating unit vectors **M** and **m** with the advancing (θ_a) and receding (θ_r) contact angles.

view, during its formation the droplet responds to changes in D_d by changing its contact angles in order to allow an interfacial force on the contact line sufficient to keep the droplet on the membrane.

The force balance model has been developed from the equation governing the equilibrium of a droplet on an inclined surface [14]. Analogous force balance equations, derived for a droplet on the membrane pore subjected to the action of a cross-flowing fluid, yield a relation between the instantaneous droplet diameters and the advancing and receding contact angles [12] (θ_a and θ_r, respectively) defined as in Fig. 3, along the contact line (Fig. 4). Following this approach it is assumed that the shape of the contact line is known (as e.g. for the circular contact lines reported in Fig. 4). For continuity between the two parts where θ_a and θ_r are considered constant, a transition zone (TZ) has to be postulated. However, this zone is assumed to be small as compared to the pore circumference.

If we consider a contact line Γ of generic size and shape, with reference to Fig. 3, the interfacial tension force can be expressed as the sum of the following two components:

$$\begin{aligned} F_{\gamma i} &= \int_{\Gamma} \gamma(\mathbf{M}\cdot\mathbf{m})\mathbf{m}\cdot\mathbf{i}\,\mathrm{d}\Gamma \quad \text{parallel to the membrane surface} \\ F_{\gamma k} &= \int_{\Gamma} \gamma(\mathbf{M}\cdot\mathbf{k})\mathbf{k}\cdot\mathbf{k}\,\mathrm{d}\Gamma \quad \text{perpendicular to the membrane surface} \end{aligned} \tag{7}$$

where **M** and **m** are the unit vectors, whose directions are indicated in Fig. 3. Concerning the shape of Γ, it shall be noted that in the general formulation of Eq. (7) the droplet contact line does not necessarily coincide with the pore border and, depending on the affinity between the membrane and the disperse phase, the droplet can slightly spread around the pore. In Eq. (7), the total **j** component (parallel to the membrane surface) is zero since symmetric contact lines are considered here. The integration along the contact line can be carried out by dividing the line into four sections: the advancing (Γ_a) and receding (Γ_r) portions, along which the contact angles assume the constant values of θ_a and θ_r, respectively, and the two lines corresponding to the transition zones (TZ) in which the contact angles are not constant (Fig. 4). Using the following definition for the contact angle:

$$\cos\theta = \mathbf{M}\cdot\mathbf{m} \tag{8}$$

Eq. (1) can be expanded as:

$$\begin{aligned} F_{\gamma i} &= \gamma\cos\theta_a \int_{\Gamma_a} \mathbf{m}\cdot\mathbf{i}\,\mathrm{d}\Gamma + \gamma\cos\theta_r \int_{\Gamma_r} \mathbf{m}\cdot\mathbf{i}\,\mathrm{d}\Gamma \\ &\quad + 2\gamma \int_{TZ} \cos\theta(\Gamma)\,\mathbf{m}\cdot\mathbf{i}\,\mathrm{d}\Gamma \\ F_{\gamma k} &= \gamma\sin\theta_a\,\Gamma_a + \gamma\sin\theta_r\,\Gamma_r + 2\gamma\int_{TZ}\sin\theta(\Gamma)\,\mathrm{d}\Gamma \end{aligned} \tag{9}$$

In the calculations presented below, the transition zone is taken as 0.1Γ and there, for continuity, θ is assumed to vary linearly between θ_a and θ_r.

According to the wetting membrane property, in this model it is possible to define two different interfacial tensions: one to be used in Eq. (9) and another in Eq. (1). The first value would take into account the interaction between the liquid–liquid interface and the membrane surface, the second one would only consider the liquid–liquid interfacial tension, according to Laplace equation. In the following calculations, one value of γ is used in both equations. This corresponds to assuming that the force balance is evaluated along a liquid–liquid interface lying on the layer of disperse liquid located in the membrane pore.

The resulting set of force balance equations is:

$$\begin{cases} F_{\gamma i}(\theta_a,\,\theta_r) + F_{DR} = 0 & \text{parallel to the membrane surface} \\ F_{\gamma k}(\theta_a,\,\theta_r) + F_{YL} + F_{DL} & \\ \quad + F_{BG} = 0 & \text{perpendicular to the membrane surface} \end{cases} \tag{10}$$

where the dependence of the interfacial tension force on the contact angles is reported for clarity. This set of equations can be solved at every droplet diameter to find the contact angles providing the equilibrium of forces.

In the present work, we illustrate a procedure adopted for solving Eq. (10), more rigorous than the one used in Ref. [12]. For given process conditions, Eq. (10) is a set of two non-linear equations in the variables θ_a, θ_r and D_d. In the mathematical

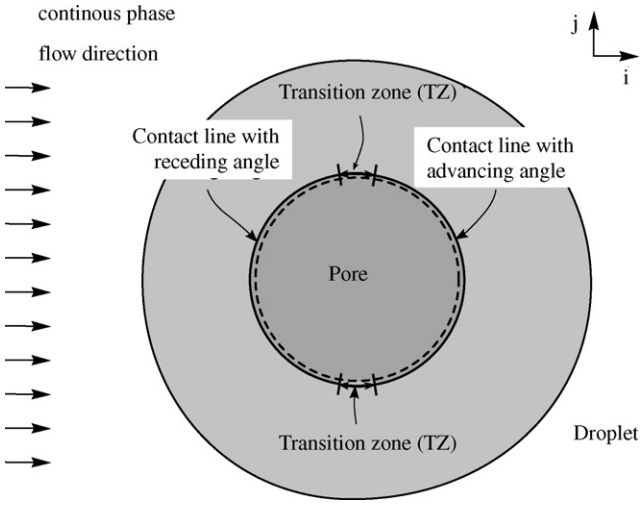

Fig. 4. Droplet on the membrane pore. Top view showing the advancing and receding contact angles and the transition zone.

solution of Eq. (10), it shall be considered that multiple or no solution can be found, or the solutions can be unacceptable from a physical point of view (i.e. $\theta_a, \theta_r \notin [0, \pi]$). Eq. (10) are solved numerically by the continuation software AUTO [15]. Starting from a known solution, this technique allows to trace the solution pathways in the space of the variables, when a given variable (called *parameter*) is changed. The approach is able to track limit points and to find multiple solutions for the same value of the parameter. In the present context, the procedure is extensively used to find the values of θ_a and θ_r for any value of the droplet diameter (chosen as parameter). The solution paths are shown to be in all cases closed lines laying within a minimum and maximum D_d value corresponding to the pore diameter (D_p) and a critical value denoted by D_c (*critical droplet diameter*), respectively. Since no solution exists for a droplet diameter larger than D_c, then it is concluded that this value has the meaning of droplet diameter corresponding to which the detachment of the droplet starts. In those cases where solution branches are found to be physically unacceptable, D_c is taken to be the smallest diameter corresponding to one of the two contact angles reaching the value of 0 or π.

It is important to stress that the D_c (from FBE) and D_d (from TBE) represent the dimension corresponding to which the force or torque balance is broken, respectively. Thus, if the detachment of the droplet occurs without necks or tails, these values correspond to the actual droplet size. However, spontaneous deformations due to surface free-energy minimization [8,9] and consequent droplet detachment can occur when the force balance at the base of the droplet or the torque balance are not broken yet, in this case D_c and D_d do not represent the final droplet size. In addition, if the balances are broken but the droplet remains nonetheless attached to the liquid in the pore with an evident tail, the calculated values can not be used again to estimate the final droplet diameter.

3. Results and discussion

There is a variety of experimental data available on membrane emulsification processes. However, to compare the model results with experimental values, some requirements on the data are necessary:

- the conditions for unhindered droplet growth on the membrane surface have to be fulfilled. Moreover, the coalescence of droplets in the continuous phase has to be absent as well;
- complete experimental data, i.e. average droplet sizes, membrane pore size (pore border morphology), emulsifiers (interfacial tensions), average cross-flow velocities (or the shear stress at the membrane surface), trans-membrane pressures (capillarity pressures), and formation times must be given;
- membrane module geometry and sizes must be reported. The module dimensions and design are extremely important to evaluate the shear stress at the membrane surface;
- structural modifications (i.e. hydrophilic and hydrophobic modifications of the membrane surface), due to membrane pre-treatment, have to be absent.

Aware of the fact that all experimental conditions are not readily available in the literature, we have selected those experimental works fulfilling as many requirements as possible. Katoh et al. [5], Vladisavljevic and Schubert [16,17] and Kobayashi et al. [18] have reported different data on oil–water emulsions, obtained with tubular and rectangular hydrophilic membranes. In particular, Katoh et al. [5] and Vladisavljevic and Schubert [16,17] used tubular hydrophilic Shirasu-porous-glass (SPG) modules, whereas Kobayashi et al. [18] employed a flat rectangular-type hydrophilic polycarbonate membrane with a mean pore diameter of 10 μm. Unfortunately, the pore border shape of the SPG membrane could not always be approximated with a circumference [19]. This has to be taken into account during the comparison of the model results with the experimental data in Refs. [16,17]. Kobayashi et al. used polycarbonate membranes that have circular pore border, as well shown from the scanning electron microscopy (SEM) image reported in their work [18]. In all cited experiments, the disperse phase fluxes are slightly higher than the corresponding capillarity pressures, therefore jets of the disperse phase should be absent. It shall be stressed that experiments in Ref. [18] at low cross-flow velocity do not totally fulfil the issue of unhindered droplet growth. All the experimental conditions are summarized in Table 1.

It shall be remarked that, although the value of γ depends on the quantity of emulsifier dynamically adsorbed on the liquid–liquid interface, in the presented results the force and torque balances are solved by using the equilibrium interfacial tension of the emulsifiers employed. In fact, in the literature, some authors [16,20] used these interfacial tension values in the Laplace equation to obtain, for the same membrane studied in this work, the capillarity pressures very close to experimental data.

Fig. 5 compares the relationships between the droplet diameter and the cross-flow velocity obtained using the two models and the corresponding experimental data [18]. The interfacial tensions are 2.5, 4.0 and 4.4 mN/m (Fig. 5a–c), respectively. When the cross-flow velocity is greater than 0.5 m/s, the results of the force balance equations approach the experimental ones for all tested interfacial tensions. At lower values of the velocity, a poor agreement is obtained for both models and the reason for this is discussed below. At high cross-flow velocities, the FBE curves present evident asymptotes, whereas, particularly in Fig. 5b and c, the TBE results show a steeper decrease of the predicted droplet diameter as the velocity increases. It is interesting to emphasise that in the experiments significantly different values are observed for a small difference of the surface tension values (4.0 mN/m versus 4.4 mN/m). This effect is likely due to the chemical nature (cationic or anionic) of the emulsifiers utilized in the two cases [18]. In fact, the surface tension of the emulsifiers has been measured by gravimetric viscosimetry, neglecting their interactions with the membrane. Moreover, the droplets obtained experimentally using PGFE and Tween 20 are larger than those achieved by using SDS. This can be due to the *dynamic* interfacial tensions of the surfactants. SDS, in fact, adsorbs more quickly on an oil–water interface than Tween 20 and PGFE. Thus, when these two emulsifiers are utilized, the actual dynamic value of interfacial tension should be used in

Table 1
Experimental conditions

Reference	Membrane	Module geometry	γ (mN/m)	v (m/s)	D_p (μm)
Katoh et al. [5]	SPG	Tubular	4[a]	0.1–0.9	0.57, 2.34
Vladisavljevic and Schubert [17]	SPG	Tubular	7[a]	1.4	0.4–6.6
Kobayashi et al. [18]	Polycarbonate	Plane	2.5, 4.0, 4.4	0.1–0.7	10

[a] Values correspond to the equilibrium tension γ_∞ available in literature [6,18,20] for SDS and Tween 80, respectively.

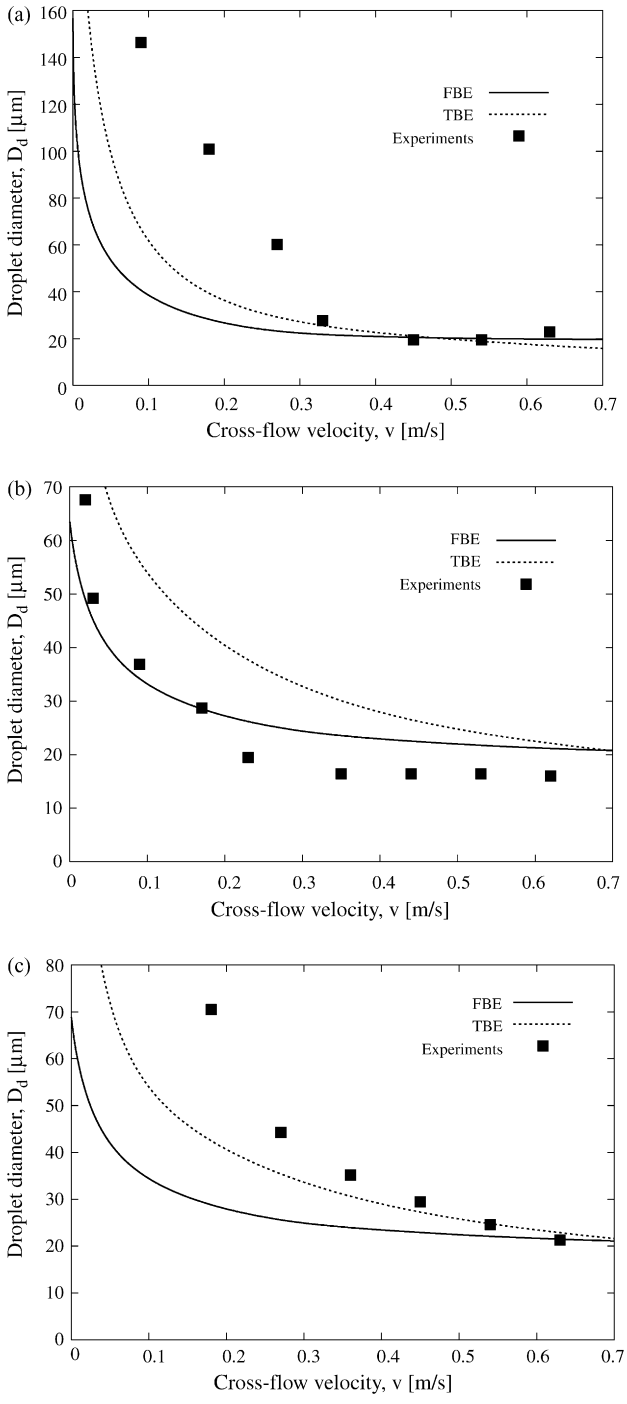

Fig. 5. Experimental data [18] and model predictions of droplet size vs. average cross-flow velocity for circular pore with diameter of 10 μm. The interfacial tension is 2.5 mN/m (a), 4.0 mN/m (b) and 4.4 mN/m (c).

calculations instead of the equilibrium tension. Since the two models are based simply on the value of γ (i.e. the equilibrium interfacial tensions), they produce similar results for the two cases. The results of the TBE shown in Fig. 5c appear in better agreement with the data than those of the FBE.

Fig. 6 shows the solutions of Eqs. (6) and (10) corresponding to cross-flow velocities ranging from 0.1 to 1 m/s. The calculations were carried out using an equilibrium interfacial tension of 4 mN/m (sodium dodecyl sulphate, SDS) and a membrane pore size of 0.57 μm. The experimental data refer to the work of Katoh et al. [5]. The droplet diameters, derived by force balance equations, are in good agreement with experimental values again for cross-flow velocities higher than 0.6 m/s, whereas the torque balance model yields a large overestimation of the experimental data in the whole range of velocities. Figs. 5 and 6 clearly show that the force-based model produces accurate predictions, though only at high cross-flow velocities. This is somewhat expected, since it is well known that, at low cross-flow velocities, large and spontaneous droplet deformations can occur before the final detachment [9,20]. For example, droplets can form as a result of the breakage of a neck [6,7] connecting the droplet with the disperse phase still in the pore. In addition, Kobayashi et al. [18] reported that droplet coalescence occurred when the emulsifier with an interfacial tension of 2.5 mN/m was used (Fig. 5a). In these cases, both models are unable to yield reliable values.

Katoh et al. [5] reported the D_d versus v correlation only for a membrane pore of 0.57 μm. However, they reported that when cross-flow velocity is greater than 0.2 m/s a mono-disperse emulsion, having droplet diameter five times greater than pore

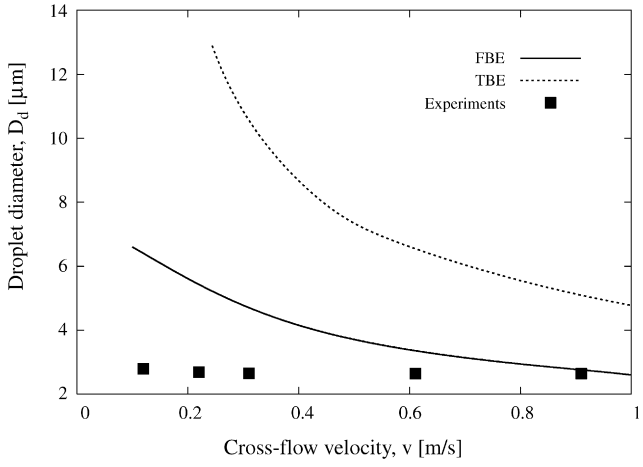

Fig. 6. Experimental data [5] and model predictions of the droplet size vs. average cross-flow velocity for a circular contact line. The interfacial tension is fixed to 4 mN/m and the pore diameter is 0.57 μm.

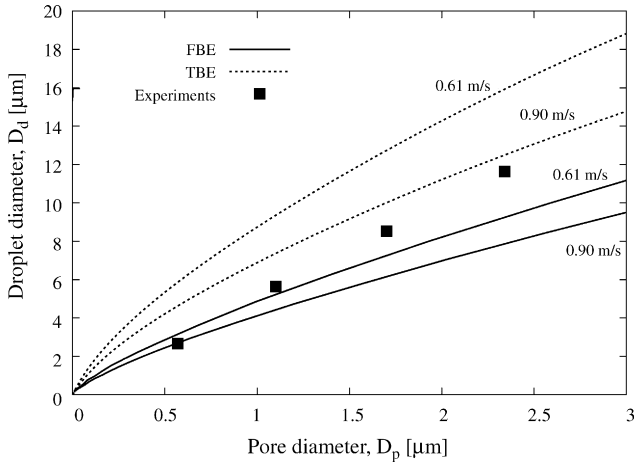

Fig. 7. Experimental data [5] and model predictions for the droplet vs. pore diameter, using an interfacial tension of 4.0 mN/m and a cross-flow velocity of 0.6 and 0.9 m/s, respectively.

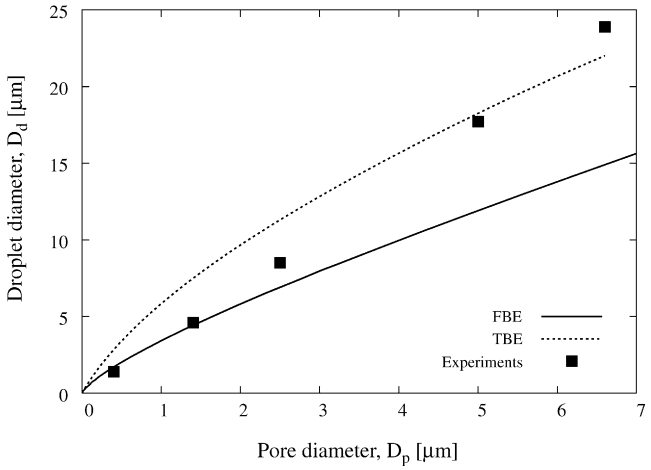

Fig. 8. Experimental data [17] and model predictions for the droplet vs. pore diameter, using an interfacial tension of 7.0 mN/m and a cross-flow velocity of 1.4 m/s.

diameters, was obtained for pore sizes ranging between 0.57 and 2.34 μm. For the highest value, this relationship gives a value of 11.7 μm for the droplet diameter. Fig. 7 shows the relationships between the droplet and pore sizes evaluated by using the two models, with an interfacial tension of 4 mN/m, and the set of experimental data [5]. In Fig. 7, the membrane pore sizes range from 0.57 to 2.34 μm and in the model the interfacial tension is set to 4 mN/m. Differently from the experiments, in these conditions the force and torque balance results are sensitive to the value of v, as clearly shown in Fig. 6. Consequently, the calculations reported in Fig. 7 are obtained using the experimental highest values of velocity (0.61 and 0.90 m/s), where the droplet diameters are less influenced by changes of cross-flow velocity. As shown in Fig. 7, using the torque balance model and a cross-flow velocity of 0.9 m/s a droplet diameter of 12.65 μm is obtained, in good agreement with the experimental value, whereas the force balance approach yields a remarkable underestimation (8.0 μm). However, Fig. 7 shows clearly that for pore sizes up to about 1.4 μm the FBE yields values in satisfactory or good agreement with the results of Katoh et al. [5], whereas the TBE gives a significant overestimation of these experimental data.

In order to discuss the poor agreement of the FBE results at large pores some considerations on the module geometry adopted are necessary. The polycarbonate membrane module used in Ref. [18] has a rectangular geometry with circular pores. Katoh et al. [5] used the same emulsifier (SDS) but tubular SPG membranes. Thus, due to the particular set-up used in Ref. [18] the calculated shear stress at the membrane surface is 7.3 Pa, whereas the shear stress in the experiments of Katoh et al., corresponding to a cross-flow velocity of 0.9 m/s, is equal to 3.4 Pa. Details of the calculation procedure for $\tau_{c,s}$ can be found in Ref. [12]. Therefore, the different agreement found in Figs. 5 and 7 for large membrane pores can be due to the different shear stresses at the membrane surfaces. In particular, for high shear stresses, the FBE yields results closer to the experimental data. However, the comparison (reported below) between models' results and experimental data obtained from Vladisavljevic and Schubert [16,17] shows that the pore border morphology also plays an important role in the reliability of the balance models presented.

The same calculations of Fig. 7 were repeated for membrane pore sizes ranging from 0.4 to 6.6 μm and using a cross-flow velocity of 1.4 m/s (Fig. 8). The simulated values are compared to the experimental droplet sizes measured by Vladisavljevic and Schubert [17] who found a linear scaling, with a slope equal to 3.5, between the droplet and pore sizes. As in the previous calculation, the force balance equations yield droplet sizes in good agreement with experimental data for small pore sizes (up to about 1.5 μm). The TBE yields a large overestimation of the droplet diameters for membrane pore sizes smaller that 2.5 μm, whereas it gives satisfactory results for large pore sizes. In these experiments, due to the velocity value, the shear stress was 7.4 Pa. This value is now comparable to the shear used by Kobayashi et al. [18]. In contrast to polycarbonate membranes, SPG membranes do not always present regular circular pores [19,21]. Therefore, as mentioned above, the poor agreement found between FBE predictions and Vladisavljevic and Schubert data, for large membrane pores, is not due to the shear stress, but may be due to the morphology of the SPG pore.

In conclusion, the various comparisons between the model predictions and experimental data show that a general agreement is not achieved. This is due to both the model assumptions and to the difficulty to compare with experimental data obtained under non-ideal conditions. Future work is necessary to improve the reliability of the predictions by removing or at least relaxing assumptions, such as the expression of the macroscopic drag force, the equilibrium value of the interfacial tension. In addition, Eq. (7), involved in the FBE model, can be solved for pore borders with shapes not circular, i.e. more similar to the actual aspects of the membrane pores used in the experiments. Also, experiments specifically designed to produce results in *idealized* conditions, useful for direct validation of the models, are highly sought. Bearing in mind the present set of investigated conditions, we can conclude that for high shear stresses (which depend on the cross-flow velocity and membrane module set-up) and for small membrane pore sizes the FBE yields droplet diam-

eters in good agreement with experimental data. This confirms the expectations based on the assumptions made in its derivation, as introduced in Section 2. In fact, for small pores and high shear stresses the droplet shape is more realistically expected to be similar to a spherical cap stuck on the corresponding pore border and distorted at its base.

4. Conclusions

In this work, we compare the reliability of two macroscopic balance models developed to analyse the formation of droplets during the cross-flow membrane emulsifications. The predictions, in terms of final droplet diameters as a function of the operating parameters and emulsification conditions, using the torque balance model and the force-based approach are compared against experimental data available in the literature.

The conclusions of this study can be summarized as follows:

- the force balance equations yield better droplet sizes than the torque balance for high shear stresses and small membrane pore sizes, depending on the interfacial tension considered. For large pore sizes, the torque balance equation is more reliable than FBE;
- the force balance model presents an asymptotic D_d versus v behaviour in better agreement with the experimental trends than the torque balance model. In particular, FBE results show an evident plateau for high cross-flow velocities;
- the two models are unable to reproduce the linear relation between the droplet and pore size observed in the experiments;
- for large pore dimensions poor agreement between the FBE and the experimental data is found. A possible explanation is that the force balance is more sensitive to the shape of pore border than the torque balance equation.

Appendix A. Nomenclature

D	diameter (m)
D_c	critical diameter (m)
F	force (N)
g	gravitational acceleration ($m\,s^{-2}$)
h	height of the droplet above the membrane surface (m)
i, **j**, **k**	unit vectors (Figs. 3 and 4)
k_x	correction factor in Eq. (4)
M, **m**	unit vectors (Fig. 3)
v	undisturbed cross-flow velocity ($m\,s^{-1}$)

Greek symbols

Γ	contact line
γ	surface tension ($N\,m^{-1}$)
μ	viscosity (Pa s)
θ	contact angle (rad)
ρ	density ($kg\,m^{-3}$)
τ	wall shear stress (Pa)

Subscripts

a	advancing
BG	buoyancy
c	continuous
d	droplet
DL	dynamic lift
DR	drag
i, k	along the i, k direction
p	pore
r	receding
s	membrane surface
YL	Young–Laplace
∞	equilibrium
γ	interfacial tension

References

[1] A.J. Gijsbertsen-Abrahamse, A. van der Padt, R.M. Boom, Status of cross-flow membrane emulsification and outlook for industrial application, J. Membr. Sci. 230 (2004) 149–159.

[2] S.M. Joscelyne, G. Trägårdh, Membrane emulsification—a literature review, J. Membr. Sci. 169 (2000) 107–159.

[3] S.J. Peng, R.A. Williams, Controlled production of emulsions using a cross-flow membrane Part I: Droplet formation from a single pore, Trans. IChemE 76 (1998) 894–901.

[4] V. Schröder, H. Schubert, Production of emulsions using microporous ceramic membranes, Colloids Surf. A: Physicochem. Eng. Aspects 152 (1999) 103–109.

[5] R. Katoh, Y. Asano, A. Furuya, S. Kazuyoshi, M. Tomita, Preparation of food emulsions using a membrane emulsification system, J. Membr. Sci. 113 (1996) 131–135.

[6] V. Schröder, O. Behrend, H. Schubert, Effect of dynamic interfacial tension on the emulsification process using microporous ceramic membranes, J. Colloid Interface Sci. 202 (1998) 334–340.

[7] A.J. Abrahamse, A. van der Padt, R.M. Boom, W.B.C. de Heij, Process fundamentals of membrane emulsification: simulation with CFD, AIChE J. 47 (2001) 1285–1291.

[8] M. Rayner, G. Trägårdh, Ch. Trägårdh, P. Dejmek, Using the surface evolver to model droplet formation processes in membrane emulsification, J. Colloid Interface Sci. 279 (2004) 175–185.

[9] M. Rayner, G. Trägårdh, C. Trägårdh, The impact of mass transfer and interfacial expansion rate on droplet size in membrane emulsification processes, Colloids Surf. A: Physicochem. Eng. Aspects 266 (2005) 1–17.

[10] S. van der Graaf, T. Nisisako, C.G.P.H. Schron, R.G.M. van der Sman, R.M. Boom, Lattice Boltzmann simulations of droplet formation in a T-shaped microchannel, Langmuir 22 (2006) 4144–4152.

[11] Z. Wang, S. Wang, S. Volker, H. Schubert, Effect of continuous phase viscosity on membrane emulsification, Chin. J. Chem. Eng. 8 (2000) 108–112.

[12] G. De Luca, E. Drioli, Force balance conditions for droplet formation in cross-flow membrane emulsifications, J. Colloid Interface Sci. 294 (2006) 436–448.

[13] M.E. O'Neil, A slow motion of viscous liquid caused by a slowly moving solid sphere, Mathematika 11 (1964) 67–74.

[14] E.B. Dussan, R.T.P. Chow, On the ability of drops or bubbles to stick to non-horizontal surfaces of solids, J. Fluid Mech. 137 (1983) 1–29.

[15] E. Doedel, A.R. Champneys, T.F. Fairgrieve, Y.A. Kuznetsov, B. Sandstede, X. Wang, Continuation and Bifurcation Software for Ordinary Differential Equations, Applied Mathematics Report, California Institute of Technology, 1997, AUTO97.

[16] G.T. Vladisavljevic, H. Schubert, Influence of process parameters on droplet size distribution in SPG membrane emulsification and stability of prepared emulsion droplets, J. Membr. Sci. 225 (2003) 15–23.

[17] G.T. Vladisavljevic, H. Schubert, Preparation and analysis of oil-in-water emulsions worth a narrow droplet size distribution using Shirasu-porous-glass (SPG) membranes, Desalination 144 (2002) 167–172.

[18] I. Kobayashi, M. Yasumo, S. Iwamoto, A. Shono, K. Satoh, M. Nakajima, Microscopic observation of emulsion droplet formation from a polycarbonate membrane, Colloids Surf. A: Physicochem. Eng. Aspects 207 (2002) 185–196.

[19] G. De Luca, A. Sindona, L. Giorno, E. Drioli, Quantitative analysis of coupling effects in cross-flow membrane emulsification, J. Membr. Sci. 229 (2004) 199–209.

[20] M. Yasumo, M. Nakajima, S. Iwamoto, T. Muryama, S. Sugiura, I. Kobayashi, A. Shono, K. Satoh, Visualization and characterization of SPG membrane emulsification, J. Membr. Sci. 210 (2002) 29–37.

[21] G.T. Vladisavljevic, M. Shimizu, T. Nakashima, Permeability of hydrophilic and hydrophobic Shirasu-porous-glass (SPG) membranes to pure liquids and its microstructure, J. Membr. Sci. 250 (2005) 69–77.